

Journal of Biomaterials Applications

<http://jba.sagepub.com>

Proliferation and Differentiation of Human Osteoblasts within 3D printed Poly-Lactic-co-Glycolic Acid Scaffolds

Zigang Ge, Lishan Wang, Boon Chin Heng, Xian-Feng Tian, Kai Lu, Victor Tai Weng
Fan, Jin Fei Yeo, Tong Cao and Eunice Tan

J Biomater Appl 2009; 23; 533 originally published online Aug 29, 2008;
DOI: 10.1177/0885328208094301

The online version of this article can be found at:
<http://jba.sagepub.com/cgi/content/abstract/23/6/533>

Published by:



<http://www.sagepublications.com>

Additional services and information for *Journal of Biomaterials Applications* can be found at:

Email Alerts: <http://jba.sagepub.com/cgi/alerts>

Subscriptions: <http://jba.sagepub.com/subscriptions>

Reprints: <http://www.sagepub.com/journalsReprints.nav>

Permissions: <http://www.sagepub.co.uk/journalsPermissions.nav>

Citations <http://jba.sagepub.com/cgi/content/refs/23/6/533>

Proliferation and Differentiation of Human Osteoblasts within 3D printed Poly-Lactic-co-Glycolic Acid Scaffolds

ZIGANG GE

Peking University, Biomedical Engineering, National University of Singapore, Oral and Maxillofacial Surgery, Singapore

LISHAN WANG

Institute of Bioengineering and Nanotechnology, Singapore

BOON CHIN HENG, XIAN-FENG TIAN, KAI LU,
VICTOR TAI WENG FAN, JIN FEI YEO AND TONG CAO*

National University of Singapore, Oral and Maxillofacial Surgery, Singapore

EUNICE TAN

National University of Singapore, Division of Bioengineering, Singapore

ABSTRACT: Bone repair and regeneration can be enhanced through implantation of biocompatible and biodegradable scaffolds, which serve primarily as osteoconductive moieties. In this study, the mechanical properties and microenvironment of 3D printed poly-lactic-co-glycolic acid (PLGA) scaffolds are examined. Additionally, the proliferation and differentiation of human fetal osteoblasts are evaluated after 3 weeks of *in vitro* culture on the scaffolds. The results showed that the PLGA scaffolds examined had mechanical properties similar to that of trabecular bone, but was still much weaker compared to cortical bone. In addition to general porosity, the PLGA scaffolds

*Author to whom correspondence should be addressed. E-mail: omscaot@nus.edu.sg
Figures 1, 3 and 5 appear in color online: <http://jba.sagepub.com>

JOURNAL OF **BIOMATERIALS APPLICATIONS** Volume 23 — May 2009

533

0885-3282/09/06 0533-15 \$10.00/0 DOI: 10.1177/0885328208094301

© SAGE Publications 2009

Los Angeles, London, New Delhi and Singapore

also had micropores within macropore walls. Cultured human osteoblasts could proliferate upon seeding on the PLGA scaffolds. Alkaline phosphatase activity and osteonectin expression of the osteoblasts cultured on the PLGA scaffolds remained stable over three weeks, whilst expression of collagen type I and osteopontin decreased. The alkaline phosphatase activity of osteoblasts cultured on PLGA scaffolds is comparable with that from two commercially-available scaffolds – OPLA and collagen scaffolds (Becton–Dickinson (BD) Inc., Franklin Lakes, NJ, USA). Hence, the results suggested that the PLGA scaffolds examined are conducive for promoting osteogenesis.

KEY WORDS: Osteoblast, scaffold, 3D printing, osteogenesis.

INTRODUCTION

Scaffolds serve primarily as osteoconductive moieties on which newly formed bone is deposited through creeping substitution from adjacent living bone [1]. Additionally, scaffolds can also serve as delivery vehicles for transplanted cells, [2] growth factors or even for gene therapy, to further enhance the regeneration process. As the natural role of bone is to provide support and protection for other organs, it is imperative to consider the appropriate mechanical strength and degradation rate of scaffolds utilized in bone repair. Multiple parameters have to be met when designing a scaffold for bone regeneration. Scaffolds with pore sizes $>300\ \mu\text{m}$ are optimal for *in vivo* osteogenesis, as they favor direct osteogenesis by allowing vascularization and adequate oxygenation [3]. While micropores are helpful for osteogenesis, [4] well-controlled micropore size is essential [5]. Gradient pore size has been reported to promote better cartilage and bone formation [6]. Regarding controlled release of proteins, another set of parameters for pore size and porosity are necessary [7]. When all these parameters have to be considered, some complex mathematical modeling have to be done [8]. Customized fabrication has become more and more recognized clinically. Although, much progress has been reported on new technologies of bone scaffold fabrication, no single fabrication technology could satisfy all requirements discussed above [9]. While conventional techniques are inadequate for fabricating customized scaffolds used in bone regeneration, [10] computer-aided rapid prototyping (RP) or solid free-form fabrication (SFF) could offer a promising alternative solution. RP fabricates structures through addition of material layers and particulates in a controlled mode, as specified by a computer program, which can integrate biodata from Computed Tomography (CT) and Magnetic Resonance Imaging (MRI) scan of patients [11]. 3D printing is one of such techniques and has been used to fabricate both ceramic [12]

and polymeric [13] scaffolds. Polymeric scaffolds have gained increasing popularity due to their ease of fabrication, cost-effectiveness, good biocompatibility, and controlled degradation rate [14]. Though 3D printing poly-lactic-co-glycolic acid (PLGA) scaffold has been evaluated for bone regeneration, only *in vivo* results have been reported without detailed study of osteoblast functionality *in vitro* [15,16].

In this study, *in vitro* proliferation and differentiation of osteoblasts within 3D printed PLGA scaffolds were evaluated, which are critical for potential bone regeneration. Theoretically high porosity is beneficial for nutrient exchange and tissue ingrowth; however, when controlled degradation and mechanical properties were integrated with general design, 60% porosity was utilized in current scaffold design. Good biocompatibility has been evaluated in a previous study, with MTT test and subsequent animal study (data not shown), so current study mainly focused on *in situ* biological performance of osteoblasts in scaffolds. Osteoblasts arise from multipotent mesenchymal progenitor cells and subsequently progress through three developmental stages of differentiation: proliferation, matrix maturation, and mineralization [17]. Besides the main secretory product type I collagen, osteoblasts also secrete other noncollagenous proteins including osteopontin, osteocalcin and bone sialoprotein. In general, gene expression of type I collagen peaks during the proliferation phase and declines thereafter, alkaline phosphatase activity peaks during the matrix formation phase and declines thereafter, while gene expression of osteopontin and osteocalcin peak during the mineralization phase [17]. In this study, we examined proliferation and differentiation of osteoblasts seeded on PLGA scaffolds, together with a time course of expression of collagen type I, osteopontin, alkaline phosphatase, and osteocalcin, after characterizing scaffolds for pore size and mechanical properties. The temporal alkaline phosphatase activity of osteoblasts seeded on different scaffolds, including OPLA and collagen scaffolds obtained from Becton–Dickinson (BD) Inc. (Franklin Lakes, NJ, USA), were also compared. The results showed that the 3D printed PLGA scaffolds can support proliferation and differentiation of osteoblasts, comparable to commercially-available scaffolds.

MATERIALS AND METHODS

Scaffold Fabrication

Raw PLGA (Purasorb, L-Lactide/Glycolide, 85;15, Purac, Nebraska, USA) and PGA (Purasorb, Poly-glycolic acid, Purac Nebraska, USA)

granules were grinded into 10 μm particles, mixed with a binder before being processed in a 3D printer (Zprinter[®] 310 PLUS, Z Corporation, USA). A solvent mixture of ethanol, acetone and De-ionized (DI) water was used as the bonding agent. PGA particles were leached with an ultrasonic cleaner and the remaining portion was annealed.

Scanning Electron Microscope

Investigation of the topography of polymeric scaffold was conducted using JEOL JSM-7400 F field emission scanning electron microscope (FESEM). The sample was vacuum dried at room temperature for 24 h, before coating with a thin layer of platinum (Pt) using a JEOL auto fine coater JFC-1600.

Mechanical Testing

The compression properties were measured with the Instron 5848 Micro Tester (Instron, MA, USA) at a constant strain rate of 1%/s. The cylinder scaffolds were compressed on two opposite flat surfaces until scaffold collapse was observed. This collapse was indicated by a sharp decrease in load. Dimensions of the scaffolds were measured with vernier callipers. The stress values were obtained by dividing the load with the cross-sectional area of the scaffold. The strain values were obtained by dividing the elongation with the gauge length of the specimen. The Young's modulus of the scaffold in compression was obtained from the gradient of the linear portion of the stress–strain curve. The compressive strength of the three scaffolds was computed from the maximum stress values before scaffold collapse occurred.

Cell Culture and Cell Seeding

Human fetal osteoblasts (CRL-11372, ATCC, VA, USA) were cultured in DMEM/F-12 (11039-021, GIBCO-Invitrogen, NY, USA) supplemented with 10% (v/v) fetal bovine serum (CH30160.03, Perbio, Hyclone, New Zealand) and 0.3 mg/mL Geneticin (G418 sulfate, GIBCO-Invitrogen, NY, USA). All cultures were incubated within a 5% CO_2 incubator set at 34°C, with culture media being changed every three days. According to the recommendations of ATCC, a temperature of 34°C instead of 37°C is optimal for the proliferation of the current human osteoblast cell line. Osteoblasts were trypsinized with trypsin-EDTA solution (T3924, Sigma, USA) when they reached 80% confluence. Two hundred thousand of osteoblasts were loaded directly onto

each PLGA scaffold (6 mm in diameter and 6 mm in height) mixed with 60 μL of Tisseel fibrin glue (Baxter Healthcare Corporation, Glendale, CA, USA), while 3D OPLA scaffolds (cylinder with diameter: 4.2–5.2 mm, height: 3.9–4.5 mm, volume: 0.039 cm^3 , #354614, Becton–Dickinson (BD) Inc., Franklin Lakes, NJ, USA) and collagen scaffolds (cylinder with diameter: 4.2–5.2 mm, height: 3.9–4.5 mm, volume: 0.039 cm^3 , #354613, Becton–Dickinson (BD) Inc., Franklin Lakes, NJ, USA) served as controls for assaying alkaline phosphatase activity. 5.0×10^5 osteoblasts were loaded in exactly the same manner for PCR analysis. Cell-scaffolds systems were cultured in 24 well plates with 1 mL of above mentioned media per well. Scaffolds were relocated into new wells with fresh media every three days, so as to avoid influence from cells not associated with the scaffolds and which were attached onto the culture plate. Supernatant was collected for assay of alkaline phosphatase activity.

MTT (Dimethylthiazolyl-diphenyl Tetrazolium Bromide Colorimetric Assay)

Human embryonic palatal mesenchymal cells (cell-line HEPM, ATCC CRL 1486) were used to assess the cytotoxicity of the PLGA scaffolds by the MTT (3-[4,5-dimethylthiazolyl-2]-2,5-diphenyl tetrazolium bromide (MTT, BDH, England) colorimetric assay methods. Polyethylene (US Pharmacopia) was used as negative control. For the MTT assay, the test materials were cut from large PLGA scaffolds into $5 \times 5 \text{ mm}^2$ samples and sterilized by autoclave at 121°C for 15 min. Cells were grown in 75 cm^2 T-flask containing Minimal Essential Medium (MEM, Gibco BRL) modified to contain 2 mm l-glutamine (Gibco BRL), 0.1 mm non-essential amino acids (Gibco BRL), 1.5 g/L sodium bicarbonate (Gibco BRL) and 10% heat-inactivated fetal bovine serum. A confluent cell monolayer was trypsinized with trypsin-EDTA solution 1:1 (Sigma) in phosphate buffered saline (PBS). Cells were suspended in complete growth medium and the cell suspension centrifuged for 10 min at 4°C , 1500 rpm. The pellet was resuspended with complete growth medium and the cell suspension was dispatched in four multiwell plates (Nunclon). Each well in 24 well-plates were filled with $100 \mu\text{L}$ of 10^5 cell/ml of cell suspension. The sterilized PLGA materials and polyethylene were placed in the wells, respectively. The plate was incubated at 37°C , 5% CO_2 and the percentage of viable cells was determined after 1 and 2 days of incubation. Twenty microliters of MTT solution (5 mg/mL) was added in each well and after 3 h of incubation at 37°C , 5% CO_2 the wells, were emptied and 150 μL of DMSO was added to each

well and the optical density at 540 nm wavelength measured to determine the percentage of viable cells. Six replicates were done for samples and negative controls.

Proliferation of Osteoblasts on PLGA Scaffolds

Proliferation of osteoblasts on PLGA scaffolds was measured with PicoGreen ds DNA Quantitation Kit (9P-11496, Molecular Probe, USA) according to manufacturer's instructions. Briefly, cell-scaffold composites were rinsed with PBS before incubation in 40 μ L of 0.1% collagenase (17104-019, type IV, GIBCO-Invitrogen, NY, USA)/0.025% trypsin solution for 8 h. After centrifugation at 300 rpm for 5 min, scaffolds and enzyme solutions were removed before 200 μ L of double distilled water were added. All samples were stored at -20°C until further analysis. For proliferation analysis, 100 μ L of the sample solution was mixed with 100 μ L of PicoGreen dye and measured at excitation and emission wavelengths of 485 nm and 535 nm, respectively, with a Genios[®] plate reader (Tecan Group Ltd, Maennedorf, Switzerland). DNA concentration was determined from a standard curve and cell numbers were estimated assuming 7.5 pg DNA/cell. Four replicates were done at each time points.

Assay of Alkaline Phosphatase Activity

The assay was performed with alkaline phosphatase yellow (pNPP) liquid substrate (A3469, Sigma-Aldrich Inc., St-Louis, MO, USA) by ELISA analysis, according to the manufacturer's instructions. Briefly, 100 μ L of supernatant were mixed with 100 μ L supernatant per well of 96 well plate and incubated for 5 min, before 50 μ L of 3N NaOH was added to stop the reaction. Absorbance values were subsequently read at 405 nm. Three replicates were done at each time point.

PCR Analysis of Collagen I, Osteopontin, ALP and Osteocalcin

Total RNA was extracted using the RNeasy Mini Kit (Qiagen Inc., Chatsworth, CA, USA), following the manufacturer's instructions. Reverse transcription reaction was performed using a PCR thermal cycler, Mycycler (Bio-Rad Inc., Hercules, CA, USA). cDNA synthesis was performed using 1000 ng of total RNA per 20 μ L reaction volume with iScript cDNA synthesis kit (1708890, Bio-Rad Inc., USA) for 5 min at 25°C , 30 min at 42°C and 5 min at 85°C . Alkaline phosphatase and osteocalcin gene expression were analyzed by conventional PCR.

Table 1. Primers used for PCR analysis.

Collagen I	For	5'-cag-ccg-ctt-cac-cta-cag-c-3'
	Rev	5'-ttt-tgt-att-caa-tca-ctg-tct-tgc-c-3'
Osteopontin	For	5'-ctc-agg-cca-gtt-gca-gcc-3'
	Rev	5'-caa-aag-caa-atc-act-gca-att-ctc-3'
GAPDH	For	5'-atg-ggg-aag-gtg-aag-gtc-g-3'
	Rev	5'-taa-aag-cag-ccc-tgg-tga-cc-3'
Osteocalcin	For	5'-atg-aga-gcc-ctc-aca-ctc-ctc-3'
	Rev	5'-gcc-gta-gaa-gcg-ccg-ata-ggc-3'
Alkaline phosphatase	For	5'-ggg-ggt-ggc-cgg-aaa-tac-at-3'

PCR amplifications for the resulting cDNA samples were performed at 95°C for 5 min, followed by 35 cycles of 30-s denaturation at 95°C, 45-s annealing at 58°C, and 60-s elongation at 72°C, and a final extension at 72°C for 5 min. In addition, all RNA samples were adjusted to yield equal amplification of β -actin (housekeeping gene) as an internal control. The amplified products were subjected to electrophoresis on 2% agarose gels and subsequently stained with ethidium bromide and photographed using the Light Imaging System (Biorad, Hercules, CA, USA). Each sample was repeated at least three times for each gene of interest. Three replicates were done at each time point. The PCR primers are listed in Table 1.

For quantitative analysis, *Col 1* and *osteopontin* gene expressions were analyzed by real-time reverse transcription–polymerase chain reaction (RT–PCR) reactions using the SYBR Green PCR Master Mix System (Qiagen, Chatsworth, CA, USA) on a PCR thermocycler Stratagene MX3000P (Stratagene Inc., La Jolla, CA, USA). cDNA samples (1 μ L for a total volume of 25 μ L per reaction) were analyzed for the gene of interest normalized to the reference housekeeping gene glyceraldehydes-3-phosphate dehydrogenase, *GAPDH*. The level of expression of each target gene was then calculated as $2^{-\Delta\Delta C_t}$. Each sample was replicated at least three times for each gene of interest. Real-time RT–PCR was performed at 95°C for 15 min followed by 40 cycles of 15-s denaturation at 94°C, 30-s annealing at 55°C, and 30-s elongation at 72°C. Three replicates were done at each time point. The PCR primers are listed in Table 1.

RESULTS

The fabricated PLGA scaffolds were white porous cylinders, 6 mm in diameter and 6 mm in height, with inter-connected tunnels (Figure 1(a)).

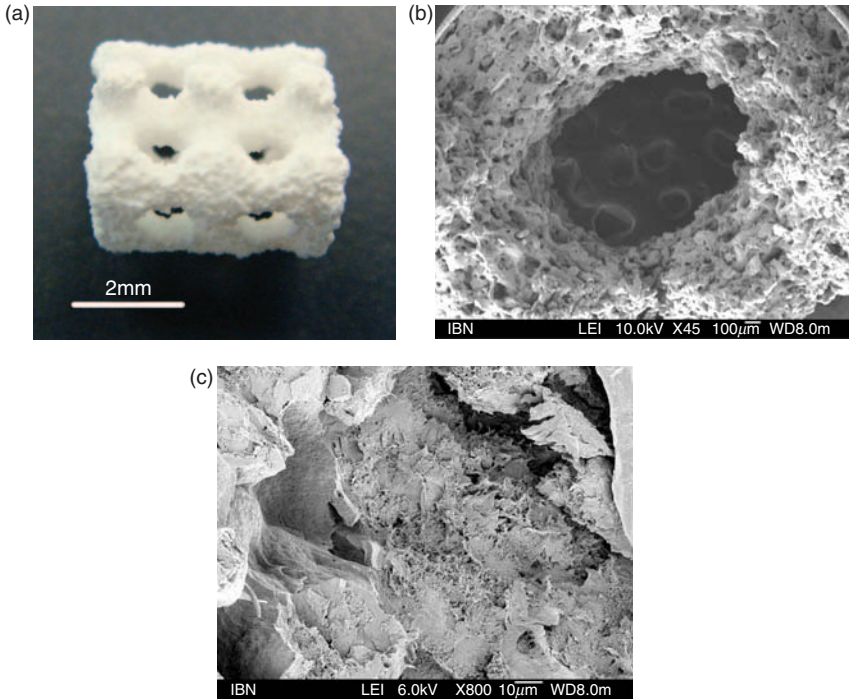


Figure 1. (a) Image of PLGA Scaffold; (b) Scanning Electronic Microscope of Scaffold; (c) Scanning Electronic Microscope of Scaffold (high Resolution).

Pore size is about 1mm and porosity is around 50% of total volume. There are large numbers of micropores within macropore walls (Figure 1(b) and (c)). The compressive strength and Young's modulus of scaffolds were 7.8 ± 3.1 MPa and 77.2 ± 10.8 MPa, respectively.

The tetrazolium-based colorimetric assay (MTT test) is a quantitative assay for the biological response of cells to a foreign body while the direct contact test permits qualitative assessment of the cells' response after exposure to PLGA materials [18]. The percentage of viable cells after exposure to PLGA materials were 95 ± 6 ($N=6$) at 24 h and 81 ± 5 ($N=6$) at 48 h, respectively, based on the percentage of viable cell referenced to 100% for the control. The 20% difference with the control was attributed to occupancy of some of the well space by the sample. Therefore, the PLGA materials were noncytotoxic to the human embryonic palatal mesenchymal cells.

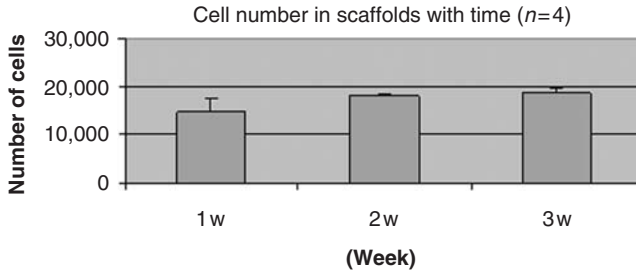


Figure 2. Proliferations of Osteoblasts in PLGA Scaffolds.

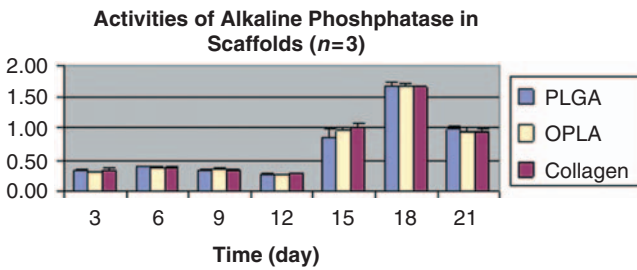


Figure 3. Activities of alkaline phosphatase of osteoblasts in PLGA Scaffolds, as well as in two commercial scaffolds, OPLA and Collagen scaffolds.

Although, some of the seeded osteoblasts continuously flowed out to culture plates during degradation of fibrin glue (data not shown), the total number of osteoblasts inside PLGA scaffolds still increased during the second week (ONE-WAY ANOVA, $P = 0.041$), but kept stable in the subsequent third week (ONE-WAY ANOVA, $P = 0.831$) (Figure 2). The alkaline phosphatase activity of osteoblasts seeded on PLGA scaffolds as well as the two commercially-available BD scaffolds (controls) were similar at all time points (Two-Way ANOVA, $F = 9$, $P = 0.827$). There was relatively low activity before 15 days, which then peaked at 18 days before subsequently decreasing (Figure 3).

When transferred from 2D culture to 3D scaffolds, the expression of both alkaline phosphatase and osteocalcin from conventional PCR remained stable at all time points (ONE-WAY ANOVA) (Figure 4). Expression of collagen I of osteoblasts from real-time PCR dropped significantly during the 1st week (ONE-WAY ANOVA, $p = 0.001$), while osteopontin expression dropped in the 2nd week (ONE-WAY ANOVA, $p = 0.040$) (Figure 5).

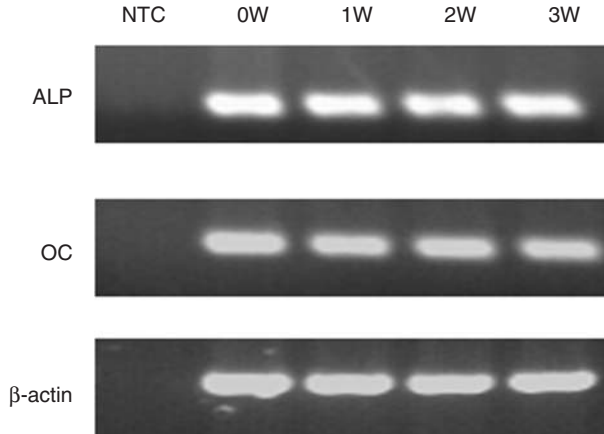


Figure 4. Expression of alkaline phosphatase and osteocalcin of Osteoblasts in PLGA Scaffolds. Note: ALP indicates alkaline phosphatase and OC indicates osteocalcin.

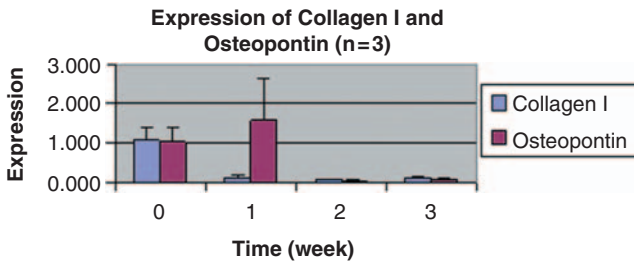


Figure 5. Expression of Collagen I and Osteopontin of Osteoblasts in PLGA Scaffolds. Note: Data at time zero indicate expression at 2D culture.

DISCUSSION

Mechanical properties of the PLGA scaffolds examined are comparable with the compressive strength (7.7 MPa) and Young's modulus (244 MPa) of human cancellous bone, [19] but are far lower than that of human cortical bone (193 MPa and 17.0 GPa, respectively) [20], Although the PLGA scaffolds are considerably stronger than most polymeric scaffolds [21–23] reported in the bone tissue-engineering field, these are still weaker than ceramic scaffolds [12]. The compressive strength of the PLGA scaffolds is 40 times higher than BD OPLA scaffolds and 1800 times higher than BD collagen scaffolds (based on information provided by BD Biosciences Labwares).

In theory, lower porosity of the scaffold stimulates osteogenesis by suppressing cell proliferation and forcing cell aggregation *in vitro*, although higher porosity and pore size result in greater bone ingrowth [9]. However, when considering potential blockage from *in vivo* tissue ingrowth, large pore size would be preferred. Forty to seventy percent volume porosity of scaffolds is generally used to attain an optimal balance of mechanical properties, controlled degradation and porosity [18,22]. The presence of micropores within macropore walls is necessary to make the material osteoinductive [4]. Based on these considerations, current scaffolds are designed with 1 mm pore size, 50% porosity and walls with rough macropores.

The surface properties of scaffold material must not only provide a passive anchoring surface, but must also be actively involved in the functionality of adherent cells, either stimulating or inhibiting them [17]. Fibrin glue is one of the most commonly used cell carriers used in cell seeding related studies, [2,24,25] however, when it is used as a cell carrier, one may presume that the seeded osteoblasts do not really come into direct contact with the PLGA scaffold surface, with the fibrin glue serving as an interface. However, under both *in vitro* and *in vivo* conditions, osteoblasts interact with biomaterials through the interfacial layer of adsorbed proteins on the scaffold surface (for example, from blood plasma, culture media, or serum) and not directly with the bare surface [26]. Thus, it would be reasonable to propose that current results are comparable to direct cell seeding without fibrin glue and with other pre-treatments used, such as culture media immersion.

The osteoblasts used in this study are from an established cell line and not from a primary explanted source. For example, they always display negative von Kossa staining even without treatment of vitamin C, dexamethasone and lipid phosphatase (data not shown). It is reasonable to assume that they may not undergo the three typical developmental stages observed during *in vitro* differentiation of primary osteoblast culture, as described previously [27]. In normal bone development and regeneration, osteoblasts are well regulated by ever-changing extracellular matrix, growth factors, as well as neural connections and blood supply, but all these factors are missing in the scaffolds which are in fact sub-optimal environments for osteoblasts. Hence, it is no surprise that expression of collagen I dropped dramatically followed by osteopontin in our real time PCR study. On the other hand, gene expression of alkaline phosphatase and osteocalcin remained rather stable in semi-quantitative conventional PCR analysis. This could be attributed to relatively less sensitive evaluation methods. Nevertheless, they can still display varying expression of osteo-specific genes upon sensing and responding

to the 3D microenvironments of different scaffolds, and hence can be used to evaluate the osteoinductive properties of scaffolds.

Alkaline phosphatase activity is important for osteoblast functionality and matrix formation [17]. Its increase therefore heralds successive osteogenic differentiation. The comparison of alkaline phosphatase activity of osteoblasts seeded on PLGA scaffolds with that on commercial scaffolds is significant. The results obtained indicate that PLGA scaffolds may have effects on osteoblasts that are similar to well-established commercially-available scaffolds [28]. Stable expression of alkaline phosphatase and osteocalcin before and after seeding on PLGA scaffolds would imply that the scaffold did not hamper the expression of these two genes and possibly did not interfere with the differentiation potential of osteoblasts. The roughness of macropores is not effective enough to increase expression of alkaline phosphatase and osteocalcin. Most of osteoinductive scaffolds are made of polymers, as well as mineral additives, which are reported to induce differentiation of osteoblasts [17].

Efficiency of cell loading was high due to a relatively large pore size and relatively small internal surface area of the PLGA scaffolds. With degradation of fibrin glue, some of the loaded cells continuously fell into the culture wells. Thus, the ascending cell numbers in the scaffolds should be a net increase after subtracting the number of cells flowing out from the scaffolds upon degradation of the fibrin glue. Seeded osteoblasts proliferated well in the 3D environment of PLGA scaffolds, but may lose some differentiation potential due to rapid proliferation, which is testified by a drop in collagen I expression [17]. As 3D environment of scaffolds provide much more surface area than 2D culture plates, the proliferation period of seeded osteoblasts may last longer than on culture plates. Expression of osteopontin was comparable in both 2D and 3D cultures. As exact functionality of osteopontin is still unclear, it is difficult to explain this trend.

CONCLUSION

The PLGA scaffolds examined are much stronger mechanically than the other two commercially-available scaffolds which served as controls. The PLGA scaffolds have similar effects on osteoblasts compared to the other two commercially-available scaffolds, with respect to expression of alkaline phosphatase activity. They can support osteoblast proliferation, as well as expression of genes important for osteogenesis, such as alkaline phosphatase, osteocalcin, collagen I, and osteopontin.

ACKNOWLEDGMENT

This study was partially supported by The Enterprise Challenge, Premier Minister Office (Singapore). The PLGA scaffolds were fabricated and provided by Bio-Scaffold International (Singapore).

REFERENCES

1. Groeneveld, E.H., van den Bergh, J.P., Holzmann, P., ten Bruggenkate, C.M., Tuinzing, D.B. and Burger, E.H. (1999). Mineralization Processes in Demineralized Bone Matrix Grafts in Human Maxillary Sinus Floor Elevations, *J. Biomed. Mater. Res.*, **48**(4): 393–402.
2. Cao, T., Ho, K.H. and Teoh, S.H. (2003). Scaffold Design and *in vitro* Study of Osteochondral Coculture in a Three-dimensional Porous Polycaprolactone Scaffold Fabricated by Fused Deposition Modeling, *Tissue Eng.*, **9**(Suppl 1): S103–112.
3. Tsuruga, E., Takita, H., Itoh, H., Wakisaka, Y. and Kuboki, Y. (1997). Pore Size of Porous Hydroxyapatite as the Cell-substratum Controls BMP-induced Osteogenesis, *J. Biochem. (Tokyo)*, **121**(2): 317–324.
4. Habibovic, P., Yuan, H., van der Valk, C.M., Meijer, G., van Blitterswijk, C.A. and de Groot, K. (2005). 3D Microenvironment as Essential Element for Osteoinduction by Biomaterials, *Biomaterials*, **26**(17): 3565–3575.
5. Lee, Y.K., Song, J., Lee, S.B., Kim, K.M., Choi, S.H., Kim, C.K., LeGeros, R.Z. and Kim, K.N. (2004). Proliferation, Differentiation, and Calcification of Preosteoblast-like MC3T3-E1 Cells Cultured onto Noncrystalline Calcium Phosphate Glass, *J. Biomed. Mater. Res. A*, **69**(1): 188–195.
6. Woodfield, T.B., Van Blitterswijk, C.A., De Wijn, J., Sims, T.J., Hollander, A.P. and Riesle, J. (2005). Polymer Scaffolds Fabricated with Pore-size Gradients as a Model for Studying the Zonal Organization within Tissue-engineered Cartilage Constructs, *Tissue Eng.*, **11**(9–10): 1297–1311.
7. Meyvis, T., De Smedt, S., Stubbe, B., Hennink, W. and Demeester, J. (2001). On the Release of Proteins from Degrading Dextran Methacrylate Hydrogels and the Correlation with the Rheologic Properties of the Hydrogels, *Pharm Res.*, **18**(11): 1593–1599.
8. Ferreira, L., Figueiredo, M.M., Gil, M.H. and Ramos, M.A. (2006). Structural analysis of Dextran-based Hydrogels Obtained Chemoenzymatically, *J. Biomed. Mater. Res. B Appl. Biomater.*, **77**(1): 55–64.
9. Karageorgiou, V. and Kaplan, D. (2005). Porosity of 3D Biomaterial Scaffolds and Osteogenesis, *Biomaterials*, **26**(27): 5474–5491.
10. Hollister, S.J. (2005). Porous Scaffold Design for Tissue Engineering, *Nat. Mater.*, **4**(7): 518–524.
11. Hutmacher, D.W., Sittinger, M. and Risbud, M.V. (2004). Scaffold-based Tissue Engineering: Rationale for Computer-aided Design and Solid Free-form Fabrication Systems, *Trends. Biotechnol.*, **22**(7): 354–362.

12. Seitz, H., Rieder, W., Irsen, S., Leukers, B. and Tille, C. (2005). Three-dimensional Printing of Porous Ceramic Scaffolds for Bone Tissue Engineering, *J. Biomed. Mater. Res. B Appl. Biomater.*, **74**(2): 782–788.
13. Dutta Roy, T., Simon, J.L., Ricci, J.L., Rekow, E.D., Thompson, V.P. and Parsons, J.R. (2003). Performance of Hydroxyapatite Bone Repair Scaffolds Created via Three-dimensional Fabrication Techniques, *J. Biomed. Mater. Res. A*, **67**(4): 1228–1237.
14. Liu, X. and Ma, P.X. (2004). Polymeric Scaffolds for Bone Tissue Engineering, *Ann. Biomed. Eng.*, **32**(3): 477–486.
15. Simon, J.L., Roy, T.D., Parsons, J.R., Rekow, E.D., Thompson, V.P., Kemnitzer, J. and Ricci, J.L. (2003). Engineered Cellular Response to Scaffold Architecture in a Rabbit Trephine Defect, *J. Biomed. Mater. Res. A*, **66**(2): 275–282.
16. Roy, T.D., Simon, J.L., Ricci, J.L., Rekow, E.D., Thompson, V.P. and Parsons, J.R. (2003). Performance of Degradable Composite Bone Repair Products Made Via Three-dimensional Fabrication Techniques, *J. Biomed. Mater. Res. A*, **66**(2): 283–291.
17. Donahue, H., Siedlechi, C. and Vogler, E. (2004). Cell Biology of the Skeletal System. In: Hollinger, J., Einhorn, T., Oll, R. and Sfeir, C. (eds), *Bone Tissue Engineering*, CRC Press, New York, pp. 43–50.
18. Ge, Z., Baguenard, S., Lim, L.Y., Wee, A. and Khor, E. (2004). Hydroxyapatite-chitin Materials as Potential Tissue Engineered bone Substitutes, *Biomaterials*, **25**(6): 1049–1058.
19. Grieb, T.A., Forng, R.Y., Stafford, R.E., Lin, J., Almeida, J., Bogdansky, S., Ronholdt, C., Drohan, W.N. and Burgess, W.H. (2005). Effective use of Optimized, High-dose (50 kGy) Gamma Irradiation for Pathogen Inactivation of Human Bone Allografts, *Biomaterials*, **26**(14): 2033–2042.
20. Reilly, D.T. and Burstein, A.H. (1975). The Elastic and Ultimate Properties of Compact Bone Tissue, *J. Biomech.*, **8**(6): 393–405.
21. Williams, J.M., Adewunmi, A., Schek, R.M., Flanagan, C.L., Krebsbach, P.H., Feinberg, S.E., Hollister, S.J. and Das, S. (2005). Bone Tissue Engineering using Polycaprolactone Scaffolds Fabricated Via Selective Laser Sintering, *Biomaterials*, **26**(23): 4817–4827.
22. Deschamps, A.A., Claase, M.B., Sleijster, W.J., de Bruijn, J.D., Grijpma, D.W. and Feijen, J. (2002). Design of Segmented Poly(ether ester) Materials and Structures for the Tissue Engineering of Bone, *J. Control Release*, **78**(1–3): 175–186.
23. Hile, D.D., Kirker-Head, C., Doherty, S.A., Kowaleski, M.P., McCool, J., Wise, D.L. and Trantolo, D.J. (2003). Mechanical Evaluation of a Porous Bone Graft Substitute Based on Poly(propylene glycol-co-fumaric acid), *J. Biomed. Mater. Res. B Appl. Biomater.*, **66**(1): 311–317.
24. Kalia, P., Blunn, G.W., Miller, J., Bhalla, A., Wiseman, M. and Coathup, M.J. (2006). Do Autologous Mesenchymal Stem Cells Augment Bone Growth and Contact to Massive Bone Tumor Implants? *Tissue Eng.*, **12**(6): 1617–1626.
25. Ge, Z., Goh, J.C. and Lee, E.H. (2005). The Effects of Bone Marrow-derived Mesenchymal Stem Cells and Fascia Wrap Application to Anterior Cruciate Ligament Tissue Engineering, *Cell Transplant*, **14**(10): 763–773.

26. Wilson, C.J., Clegg, R.E., Leavesley, D.I. and Percy, M.J. (2005). Mediation of Biomaterial-cell interactions by Adsorbed Proteins: A Review, *Tissue Eng.*, **11**(1-2): 1-18.
27. Rumpler, M., Woesz, A., Varga, F., Manjubala, I., Klaushofer, K. and Fratzl, P. (2007). Three-dimensional Growth Behavior of Osteoblasts on Biomimetic Hydroxylapatite Scaffolds, *J. Biomed. Mater. Res. A*, **81**(1): 40-50.
28. Duplomb, L., Dagouassat, M., Jourdon, P. and Heymann, D. (2007). Concise Review: Embryonic Stem Cells: A New Tool to Study Osteoblast and Osteoclast Differentiation, *Stem Cells*, **25**(3): 544-552.